# Nanoscaled Surface Modification of Poly(dimethylsiloxane) Using Carbon Nanotubes for Enhanced Oil and Organic Solvent Absorption

Chong Cheen Ong,[†] Satisvar Sundera Murthe,[†] Norani Muti Mohamed,[†,‡] Veeradasan Perumal,[‡,§] and Mohamed Shuaib Mohamed Saheed[*,†,‡]

[†]Department of Fundamental & Applied Sciences, [‡]Centre of Innovative Nanostructures & Nanodevices (COINN), and [§]Department of Mechanical Engineering, Universiti Teknologi PETRONAS, 32610 Seri Iskandar, Perak Darul Ridzuan, Malaysia

**S** *Supporting Information*

**ABSTRACT:** This article demonstrates a novel nanoscale surface modification method to enhance the selectivity of porous poly-(dimethylsiloxane) (PDMS) in removing oil from water. The surface modification method is simple and low cost by using sugar as a sacrificial template for temporal adhering of carbon nanotubes (CNT) before addition of PDMS prepolymer to encapsulate the CNT on its surface once polymerized. The PDMS−CNT demonstrated a tremendous increase in absorption capacity up to 3-fold compared to previously reported absorbents composed solely of PDMS. Besides showcasing excellent absorption capacity, the PDMS−CNT also shows a faster absorption rate (25 s) as compared to that of pure PDMS (40 s). The enhanced absorption rate is due to the incorporation of CNT, which roughens the surface of the polymer at the nanoscale and lowers the surface energy of porous PDMS while at the same time increasing the absorbent hydrophobicity and oleophilicity. This property makes the absorbent unique in absorbing only oil but repelling water at the same time. The PDMS−CNT is an excellent absorbent material with outstanding recyclability and selectivity for removing oil from water.
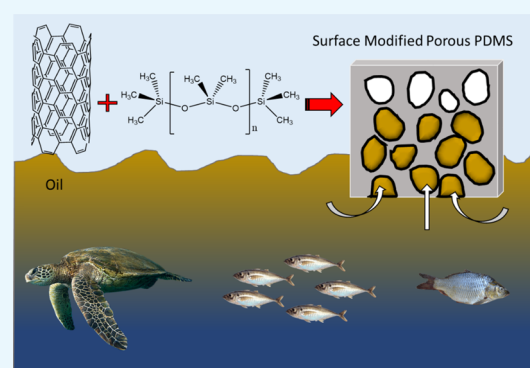
## INTRODUCTION

Oil spillage and discharge of harmful organic solvents from industries into water bodies pose a great threat to the environment, particularly to the fragile marine life. Although prevention of oil spill mishaps at sea is preferred, there are still numerous possibilities of human errors that lead to accidents. Regulatory bodies are often unable to completely monitor illegal dumping of organic solvents into water bodies. The largest oil spill at the Gulf of Mexico in 2010 has adversely affected aquatic and avian life as well as human life.[1] The presence of an oil layer on the surface of water prevents light penetration and oxygen diffusion that are crucial for the survival of marine life. Carcinogenicity and mutagenicity of these pollutants are also major threats to the aquatic population presiding in the ocean and the people living near the coastline.[2]

Current conventional methods employed in oil spill cleanup are oil skimming, in situ burning, and bioremediation. However, these methods have drawbacks such as being time consuming, high inc cost, leading to secondary pollution, or being unable to completely recover the spilled oil. As an alternative to these suboptimal methods, sorbent materials attract interest as an effective means to selectively absorb spilled oil from water due to the simple process and

efficacy.[3−6] An ideal absorbent material should be hydrophobic and oleophilic for selective oil−water separation, mechanically stable, highly porous, have a high absorption capacity, and possess good recyclability.

In recent times, researches were focused on nanomaterials such as aerogels,[7−10] graphene,[11−14] carbon nanotubes (CNT),[15,16] electrospun fibers,[3,17] and magnetic nanoparticles.[16,18] Although these nanomaterial-based absorbents show promising outcomes, the utilization of nanomaterial solely for a large-scale purpose will be expensive, complex, and time consuming. Alternatively, the process can be simplified by incorporating nanomaterials on the surface of polymer to form smart selective absorbent. Carbon-based nanomaterials are an excellent candidate to form this smart selective absorbent due to their excellent hydrophobic property, high absorption capacity, and environment friendly properties. Among the many nanomaterials, CNTs took the spotlight as the material of interest because of their efficacy in absorbing a wide range of organic and inorganic solvents due to their capabilities of chemical−nanotube interactions, high absorption capacity,
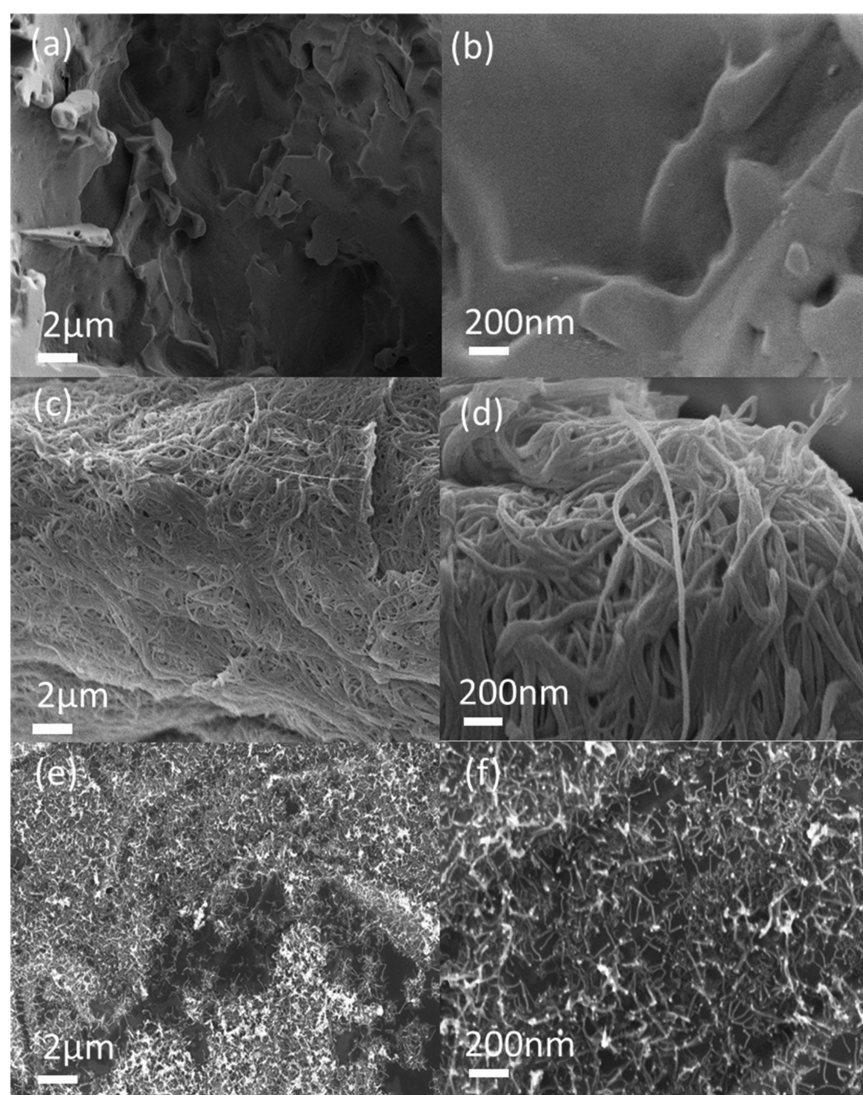
**Figure 1.** FESEM image of (a, b) cross-sectioned porous PDMS (c, d) cross-sectioned PC10, and (e, f) standalone CNT.

rapid uptake rate, tailored surface chemistry, and natural state of hydrophobicity.[15] CNT powder can be easily synthesized through chemical vapor deposition using suitable metal catalysts and carbon sources. However, to develop robust interconnected CNT in bulk scale requires expensive equipment and sophisticated steps.[16]

Therefore, to overcome such limitations, a simple surface-modified absorbent is proposed by incorporating CNT on porous poly(dimethylsiloxane) (PDMS) polymer. PDMS was synthesized as a base structure, holding the evenly dispersed CNT, giving it excellent flexibility and mechanical strength. The simple and cost-effective method to fabricate PDMS makes it a highly valuable material to be developed as a base structure. PDMS itself had been used by researchers[19,20] as an absorbent of high potential for the uptake oil and various solvents.

Despite the promising potential of PDMS, there is the intermittent water absorption problem due to water adherence on the surface of PDMS that could affect its capability. The limitation of the polymer was overcome by increasing the surface roughness through the incorporation of CNTs, which possess a large surface area and are highly hydrophobic and oleophilic.[21−23] Surface roughness is crucial in improving the

hydrophobicity and its importance can be proven by Wenzel's equation and the Cassie−Baxter equation. Besides that, CNT is also capable of lowering the surface energy, leading to greater hydrophobicity, as described in Young's equation. In this study, we demonstrated a simple method to address the issues faced by individual nanomaterials and polymers by modifying the surface of porous PDMS with CNTs where the strength of CNTs will compensate the shortcomings of PDMS and vice versa. CNTs were transferred onto the PDMS surface using a temporal sugar template. Once PDMS is polymerized, the sugar template was removed, leaving the CNTs on the PDMS surface, creating an improved hydrophobic PDMS surface. All fabrication processes were carried out in atmospheric pressure and room temperature. This modified PDMS surface can be used as it is without further modification, similar to the sponge function of absorbing oil. In our case, the sponge repels water and only absorbs to maximize the absorption capability. In our perception, this simple and inexpensive surface modification method demonstrated a promising absorbent that can be scaled-up to solve oil spill issues.
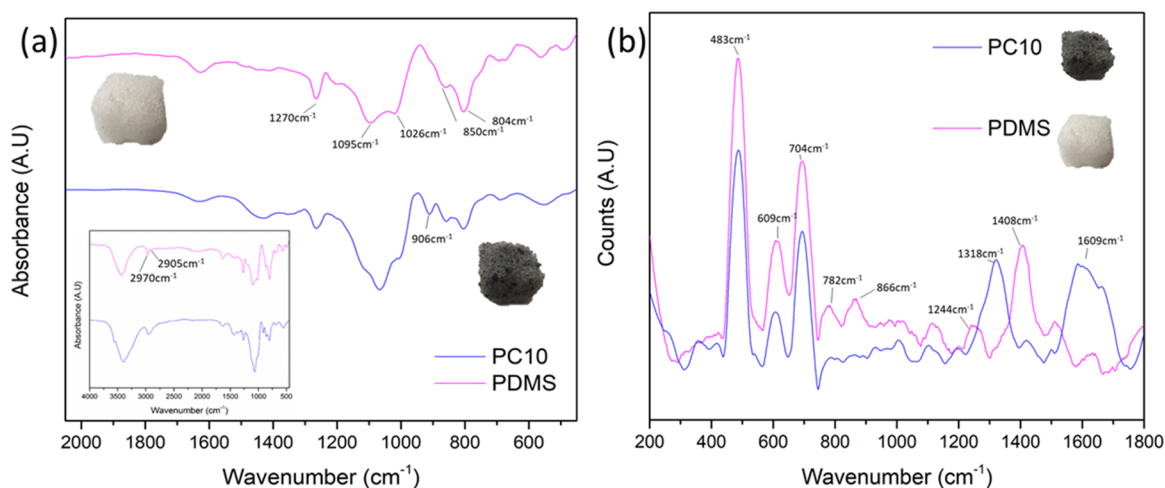
**Figure 2.** (a) FTIR spectra of PDMS and PDMS−CNT at the peak of focus (400−2100 cm$^{-1}$). Inset shows the overall FTIR spectra. (b) Raman spectra for porous PDMS and PC10 comparison.
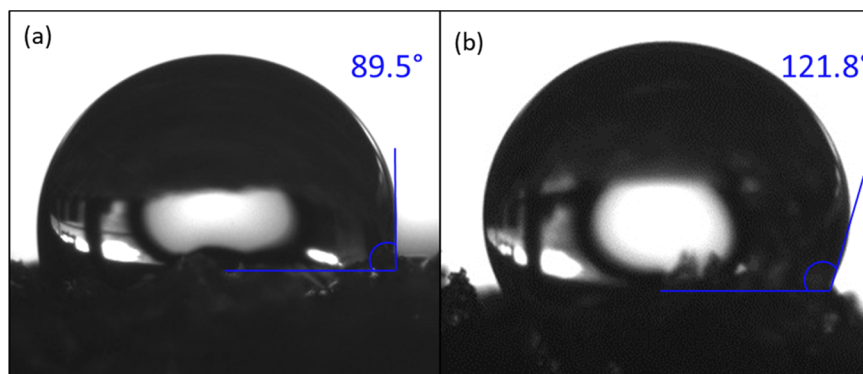


**Figure 3.** Contact angle measured on surface of (a) pure porous PDMS and (b) PC10.

## RESULTS AND DISCUSSION

To investigate the effect of CNT on the oil absorption capacity, the surface was modified using various CNT concentrations (0.2−10 mg mL$^{-1}$) in preparing the absorbent material. PDMS containing 10 mg mL$^{-1}$ of CNT (PC10) exhibited the highest absorption capacity and was selected for further study. Any further addition of CNT leads to the removal of excess CNT during the ultrasonication. A systematic study on the hydrophobicity and absorption of different types of oil and organic solvent was done to characterize the properties of the absorbent material.

**Characterization of PDMS−CNT Absorbent.** Figure 1 shows the cross-sectional field emission scanning electron microscopy (FESEM) images of the PDMS and PC10. The CNT binding on the surface of porous PC10 forms noodlelike structures which are tightly packed to each other. At lower concentrations of CNT, there are free spaces on the surface of PDMS that are available for CNT binding, as shown in Figure S1. The agglomeration of CNT observed in Figure 1d is due to the presence of van der Waals forces between CNT. In contrast to commercial powdered CNTs, CNTs in Figure 1e,f are loosely packed and further apart from each other, due to the weaker Van der Waals forces between the carbon nanotubes. The smooth surface of porous PDMS seen in Figure 1a,b is substantially roughened by the presence of CNTs, as can be seen in Figure 1c,d, which leads to improved

hydrophobicity, as proven by Wenzel's equation and the Cassie−Baxter equation (eqs S1 and S2).[24]

Figure 2a illustrates the Fourier transform infrared (FTIR) spectra of PDMS and −PC10. The asymmetric and symmetric peaks at 2905 and 2970 cm$^{-1}$ show −CH$_3$ stretching in ≡Si−CH$_3$. The presence of −CH$_3$ deformation vibration in PDMS can also be seen at the 1400 and 1270 cm$^{-1}$ peak. Besides that, peaks are also present in the 930−1200 cm$^{-1}$ range and show the presence of Si−O−Si stretching or deformation.[25,26] Peaks at 850 and 804 cm$^{-1}$ show the presence of Si−C bands and Si(CH$_3$)$_2$ rocking.[27,28] A clear difference can be observed between PDMS and PC10 at 906 cm$^{-1}$, where the PC10 shows a sharp peak with lower intensity compared with PDMS. As reported earlier,[24] this may be due to the presence of Si−C bonds between CNT and the porous PDMS structure.

Raman spectrum of porous PDMS is shown in Figure 2b. Peaks are similar to previously reported works on PDMS spectra.[25,27] The peaks consist mainly of Si−O−Si symmetrical peak at 483 cm$^{-1}$ and Si−CH$_3$ symmetric rocking peak at 609 cm$^{-1}$. The presence of Si−C asymmetric stretching at 704 cm$^{-1}$ and CH$_3$ symmetric rocking can be seen at 782 cm$^{-1}$. Besides that, CH$_3$ symmetric rocking appears at 866 cm$^{-1}$ and CH$_3$ symmetric bending appears at 1244 cm$^{-1}$. CH$_3$ asymmetric bending can also be seen at 1402 cm$^{-1}$. Generally, the intensity of the PDMS peaks is reduced with the presence of CNT. CNT peaks have been studied, and band assignments were identified in previous studies.[29−31] Characteristic peaks of
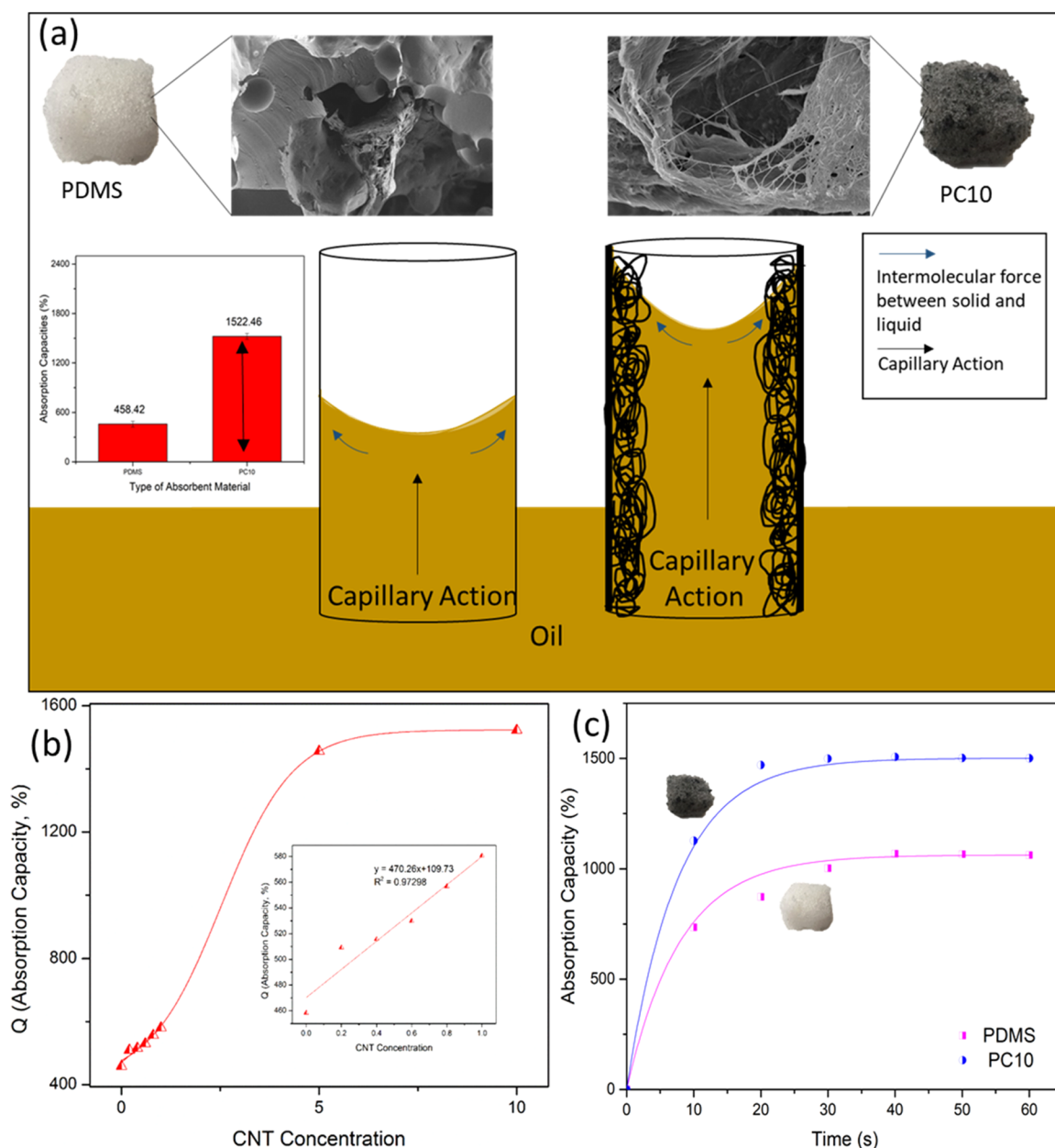
**Figure 4.** (a) Schematic illustration of comparison of capillary action between PDMS and PC10 on the basis of their FESEM images. Inset: Bar diagram shows the effect of CNT in improving absorption capacity. (b) Absorption capacity changes with different CNT concentrations. Inset: linear regression of concentration-dependent absorption capacities. (c) Comparison of kinetic absorption between PDMS and PC10.

carbon materials exist between 1000 and 1800 cm$^{-1}$ in Raman spectra for excitation energy in the visible and infrared spectrum. In this study, green (514 nm) laser radiation was used and indicates the presence of D band (disorder band) and wide G band at 1318 and 1609 cm$^{-1}$, respectively. The disentanglement of the CNT and polymer infiltration into CNT bundles explains the wide G band peak shown in Figure 2b. The intensity ratio of D to G bands is low due to the usage of green laser radiation. The intensity of G bands can be increased by switching to red laser radiation.[31]

X-ray photoelectron spectroscopy (XPS) analysis in Figure S2 indicates that the main elements of PDMS and PC10 are carbon, silicon, and oxygen. The carbon content shows significant increase from 47.64 to 63.86% for PC10. The increase in carbon element lowers the surface energy for the PDMS−CNT,[12,32] which leads to increase in contact angle, as proposed in Young's equation shown (eq S3).[33,34] It also can be observed that the intensity of Si 2s and 2p peaks is reduced with the addition of CNT to the PDMS. This is because the magnitude of the silicon to oxygen bond is greatly reduced as the amount of Si−C bonds increases with the presence of CNT.

**Surface Wetting Property.** A higher contact angle (121.8°) of PC10 (Figure 3b) as compared to that of the pure porous PDMS (89.5°) (Figure 3a) can be seen, suggesting that the presence of CNT increases the hydrophobicity. Generally, pure porous PDMS is hydrophobic by nature (Table S1). However, it exhibits intermittent hydrophilic−hydrophobic properties, where water adheres to the surface of the pure porous PDMS when forcefully immersed in water. On the other hand, water droplets do not adhere to the surface of PC10 and can be easily shaken off. PC10 contact

angle shows increments of up to 32.3° due to the presence of CNTs that enhance the surface roughness and lower the surface energy. The enhanced surface roughness traps gas molecules in the asperity valleys. This leads to disruption of the interface between solid and liquid continuity and formation of alternate solid−liquid and gas−liquid interfaces.[35] This phenomenon makes water hard to penetrate the rough surface asperities. The surface energy determines the forces of attraction or repulsion of a surface on the liquid. If the surface energy is lower than surface tension of liquid, the liquid can maintain its droplet shape. Since water has high surface tension, it will form a droplet on the surface. Comparatively, PC10 has lower surface energy than that of PDMS; therefore, the water droplet contact angle is higher. In contrast, oil derivatives having lower surface tension than the surface energy will spread over the solid surface. This is because the surface energy overpowers the oil surface tension, preventing it from forming a droplet and spread over the solid surface.

**Removal of Oil and Organic Solvents.** The removal of oil was investigated by measuring the amount of oil uptake per gram of PC10. Visual inspection revealed obvious swelling and increased volume, suggesting that the mechanism of removal is by absorption rather than adsorption. Oil was absorbed into porous PC10 structure by capillary action, and the rise and fall of liquid can be described using Jurin's law as follows

$$h = \frac{2\gamma \, \cos \theta}{\rho g r} \tag{1}$$

where $h$ is the height of liquid absorbed, $\gamma$ is the surface tension, $\theta$ is the contact angle of the liquid on the tube wall, $\rho$ is the density of the liquid, $g$ is gravity acceleration, and $r$ is the radius of tube. This law suggests that the presence of fibrous CNT within the pores facilitates the capillary action by reducing the radius of the pore. Figure 4a illustrates that presence of CNT on the surface of the inner pores reduces the radius for better oil uptake. The oil absorption performance can be observed in the inset of Figure 4a. The bar diagram reveals the performance comparison of pure PDMS and PC10 on the basis of absorption capacity. PC10 rises 3-fold compared with PDMS, showing the influence of CNT facilitates oil trapping in the porous matrix.

To further verify the effect of CNTs on oil absorption, different concentrations of CNTs were utilized before the molding process. As can be seen in Figure 4b, the absorption capacity increases as the concentration increases in almost a linear manner until it reaches saturation at approximately 6 mg mL$^{-1}$. The inset in Figure 4b shows the linear increment of percentage absorption capacity, suggesting that more CNTs are occupying the empty PDMS surface. The minute increment from 6 to 10 mg mL$^{-1}$ is to fully occupy the spaces of the porous PDMS. Excess CNTs beyond 10 mg mL$^{-1}$ are removed during sonication process, indicating that CNTs had fully occupied the spaces between the porous PDMS. Besides that, CNT also improves the absorption time upon contact with petrol. As seen in Figure 4c, PC10 only takes approximately only 25 s to achieve saturation whereas pure porous PDMS takes approximately 40 s. Petrol was absorbed into the PDMS and PC10 structure through capillary action and maintained in the porous structure by Van der Waals forces. Rapid surface wetting of PC10 can be related to the low surface energy due to presence of more carbon element.

Besides that, the surface roughness of PC10 also influences the rapid surface wetting due to larger surface area contact.

PC10 was tested further on various other organic solvents and oil. This work could achieve absorption capacities ranging from 1300 to 3100% depending on the type of absorbate. Various types of organic solvents and oils with different densities and viscosities, such as cyclohexane, diesel oil, toluene, engine oil, vegetable oil, chlorobenzene, dichloromethane, and chloroform, were used. As shown in Figure 5, the
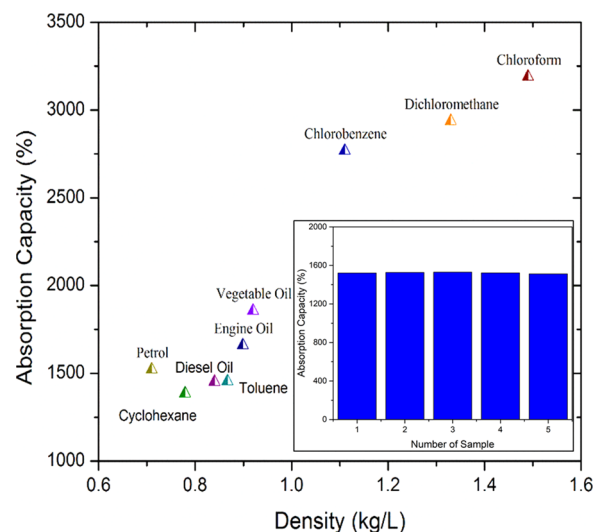


**Figure 5.** Demonstration of the absorption capacities of various absorbates of different densities. Inset: reproducibility performance of PC10.

density of the absorbate influences the absorption capacity of the absorbent material. High-density solvents such as chloroform could achieve up to 31 times the weight, whereas low-density solvents such as petrol could absorb only ∼15 times the weight. The difference is attributed to the mass of absorbate over the same volume, which is lower in low-density absorbates, hence influencing the final mass of the absorbent material. A study was conducted to prove this phenomenon by placing PC10 in 8 mL of chloroform and of petrol. It is observed that both 8 mL absorbates were absorbed into the absorbent material and produced different absorption capacities. The difference is due to chloroform having a higher density compared to that of petrol, which leads to higher mass gain by PC10. Therefore, the limiting factor on the amount of absorbate that can be absorbed is the volume. Interestingly, it was also observed that the PDMS−CNT could absorb polar absorbates such as dichloromethane, chlorobenzene, and toluene besides nonpolar absorbates. This opens new avenues for PDMS−CNT absorbent to be used in cleaning harmful organic solvents besides oil spills.

The reproducibility of the PC10 absorbent shown in Figure 5 inset has the relative standard deviation of 0.46% with similar conditions of fabrication technique and material. This reproducibility data demonstrates a consistency in oil absorption performance due to ease in controlling the fabrication condition and parameter. A comparison of previous works on absorbent-related material is shown in Table 1. Although the absorption capacity of nanomaterial shows great superiority over the current work in terms of absorption capacity, the simple and cost-effective method of developing

**Table 1. Comparison of Absorption Capacities from Studies in Previous Works on Absorbent Material**

| absorbent material | preparation method | absorption capacities (%) | author/year |
|---|---|---|---|
| poly(dimethylsiloxane) sponge | polymerization | 1100 | Choi et al. (2011) |
| magnetic carbon nanotubes | chemical vapor deposition | 5600 | Gui et al. (2013) |
| graphene-coated cotton | dip coating | 500 | Ge et al. (2014) |
| hard template PDMS | polymerization | 1301 | Zhao et al. (2014) |
| polyurethane@$Fe_3O_4$@$SiO_2$@fluoropolymer sponges | dip coating | 4450 | Wu et al. (2015) |
| $Fe_3O_4$ nanoparticle-decorated 3D graphene aerogels | nonaqueous solvothermal method | 2000 | Li et al. (2016) |
| superhydrophobic magnetic polyurethane sponge | dip coating | >3000 | Beshkar et al. (2017) |
| PDMS−CNT | surface-functionalized polymerization | 3100 | current work |
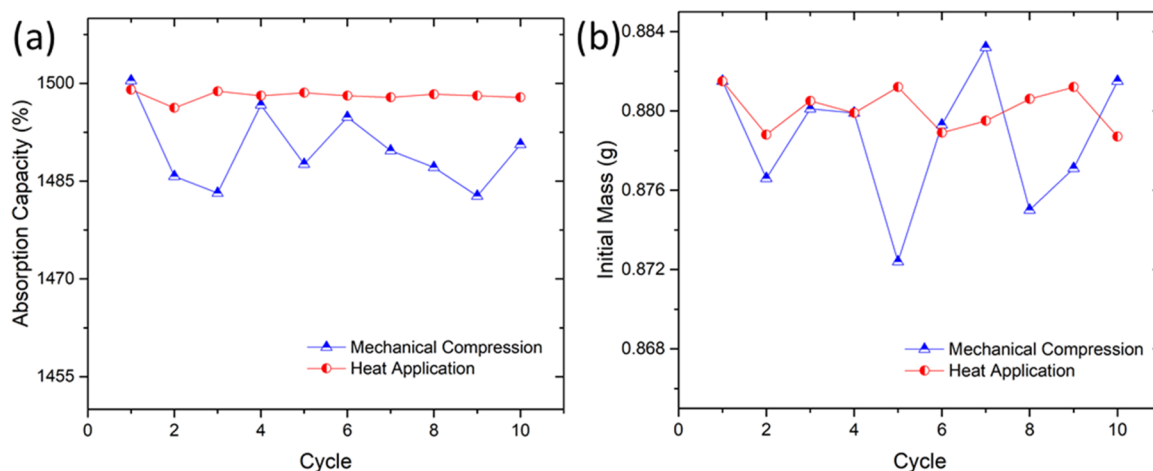


**Figure 6.** (a) Showing the recyclability on absorption capacity. (b) Initial mass changes per cycle.
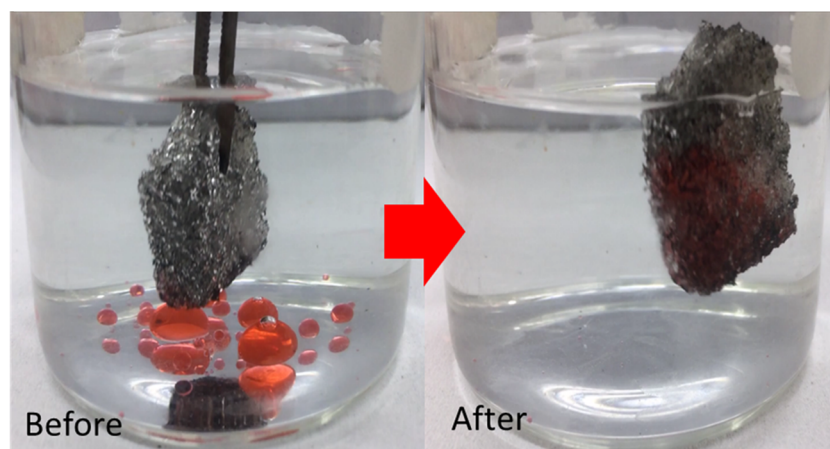


**Figure 7.** Removal of chloroform dyed with Sudan III by PDMS−CNT absorbent material.

PC10 is much favorable for large-scale development. This PC10 acts as a bridge between polymer and nanomaterials to compensate the shortcoming of each material, whereby CNT as nanomaterial improves the absorption of oil and PDMS as polymer improves the flexibility and mechanical strength using a cheap and simple method. Ultimately, PC10 shows the best of both worlds in removal of oil and organic solvent applications. A more detailed comparison of previous works is shown in Table S2.

**Analytical Performance of Absorbent, Recyclability, and Selectivity.** An ideal absorbent includes the ability to recover the absorbate to be reused, i.e., the ability to be used repeatedly without diminishing the performance. Figure 6a shows comparison between the effect of heat application and mechanical compression on the percentage absorption capacity. Clearly, it can be seen that the heat application possesses consistent absorption capacity per cycle compared with mechanical compression. This is attributed to the inconsistency of the absorbent in returning to its initial mass after mechanical compression, as shown in Figure 6b. This may be due to trapping of oil inside the absorbent material after compression that influences the absorption capacity of the following cycle. In terms of selectivity, we dropped chloroform that was dyed with Sudan III into a beaker filled with tap water, followed by absorption of oil using PC10. PC10 was observed to be able to absorb the chloroform immediately upon contact and remained floating on the water, as shown in Figure 7 due to its hydrophobic property (121.8°). As reported earlier, when porous PDMS is immersed in water, water adheres to the surface. In this study, the water does not adhere to the surface
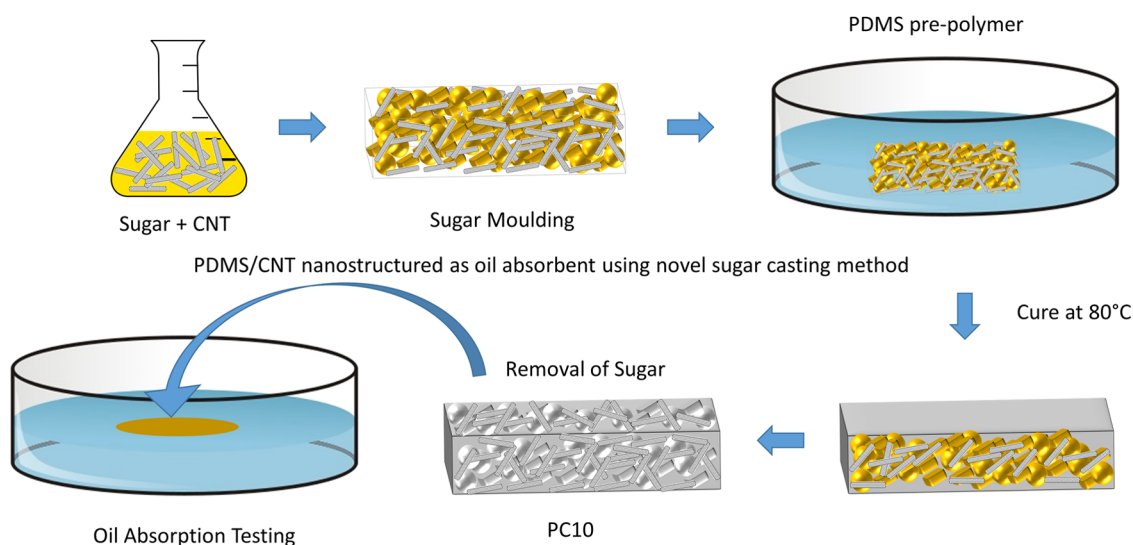
**Figure 8.** Schematic illustration of PDMS and PC10 preparation.

due to the presence of CNTs that increased the hydrophobicity. Water droplets on PC10 absorbent can be easily removed by shaking off from the surface without wiping the surface. The selectivity and recyclability of this PC10 makes an excellent absorbent material to be used not only for oil spill recovery but also for various organic solvent remediations.

## CONCLUSIONS

A simple and inexpensive novel method to modify the surface of PDMS using CNTs has been demonstrated. CNTs are successfully transferred on the surface of PDMS from a sacrificial sugar template, forming uniform distribution of CNT in noodlelike structure throughout the pores of PDMS. The effect of the amount of CNT concentration on the performance of oil absorption was investigated. The decoration of CNT enhances the absorption capacity to 3100%, which is 3-fold higher than that in a previously reported study on pure PDMS. With the inclusion of CNT, the absorbent shows rapid absorption and improved hydrophobicity from 89.5 to 121.8°, leading to enhanced selective removal of oil from water. The ability to be reuse, recycle, and recover makes it an excellent cost-effective absorbent material. The absorption is not only limited to oil derivatives but also can be extended to various polar and nonpolar organic solvents. Moreover, the PC10 demonstrated excellent recyclability property using two different methods which were mechanical compression and heat application. The strategy proposed in this study using surface-modified PDMS with CNT, also opens a new avenue to be applied in industrial waste water treatment system by removing harmful solvents before release to the environment.

## EXPERIMENTAL SECTION

**Material and Reagent.** PDMS and thermal curing agent (Sylgard 184 Silicone Elastomer Kit) were purchased from Dow Corning (Michigan). Carbon nanotubes (TUBALL) were purchased from OCSiAl (Luxembourg). Acetone, chloroform, cyclohexane, toluene, cholorobenzene, and dichloromethane were purchased from Sigma-Aldrich (Missouri). Petrol, engine oil, and diesel oil were purchased from Petronas Sdn Bhd (Kuala Lumpur, Malaysia). Vegetable oil and sugar were purchased from local shops. All reagents were stored as per supplier recommendations.

**Carbon Nanotube Solution Preparation.** CNT was dispersed in acetone solution using a tip sonicator for 30 min for even distribution of the carbon nanotubes. To study the effect of CNT in oil absorption application, various concentrations of CNT solution are prepared by altering CNT mass (0.1, 0.2, 0.4, 0.6, 0.8, 1, 5, and 10 mg mL$^{-1}$) but keeping the volume of solvent constant (1 mL).

**Absorbent Material Preparation.** One milliliter of 10 mg mL$^{-1}$ CNT solution was evenly dispersed and mixed with 2.5 g of sugar, then dried in an oven at 150 °C for 1 h to remove solvent. The sugar mixture was then kneaded by adding a few drops of water and casted into molds (1 cm × 1 cm × 1 cm), as shown in Figure 8. The molds were then dried in the oven at 100 °C for 1 h to form the sugar template. A mixture of PDMS was prepared on a Petri dish by mixing PDMS prepolymer and thermal curing agent in a ratio of 10:1 (w/w) and degassed for 3 h. The sugar template was then placed in a mixture of PDMS solution. The mixture of PDMS penetrates the sugar template using capillary forces. The sugar template with absorbed mixture was then cured at 80 °C for 2 h to complete the polymerization. After curing, the sugar template was removed by dissolving it in water at 40 °C and sonicated to remove the remaining sugar template to form PDMS/CNT(PC10) surface-modified absorbent. These steps were repeated using different concentrations: 0.1 (PC0.1), 0.2 (PC0.2), 0.4 (PC0.4), 0.6 (PC0.6), 0.8 (PC0.8), 1 (PC1), and 5 (PC5).

**Characterization of Absorbent Material.** The cross-sectional morphology of the PDMS and PDMS−CNT was analyzed using a variable pressure field emission scanning electron microscope (VPFESEM, Zeiss Supra55 VP). PDMS−CNT was coated with gold to prevent a charging effect, and samples images were captured under a low beam voltage (5 kV). To verify the bonding of the CNT on the surface of PDMS, Fourier transform infrared spectroscopy (FTIR, Model: Pelkin Elmer, Spectrum One) analysis was used. To further verify the presence of CNT on the PDMS, Raman spectroscopy (Horiba Scientific) was conducted at 514 nm. The surface chemical composition was obtained using X-ray photoelectron spectroscopy (XPS Model: Thermo Scientific, K-Alpha) with a monochromatic Al K$\alpha_1$ source of 1593 eV. The ramé-hart contact angle goniometer was used to determine the water contact angle directly by capturing the
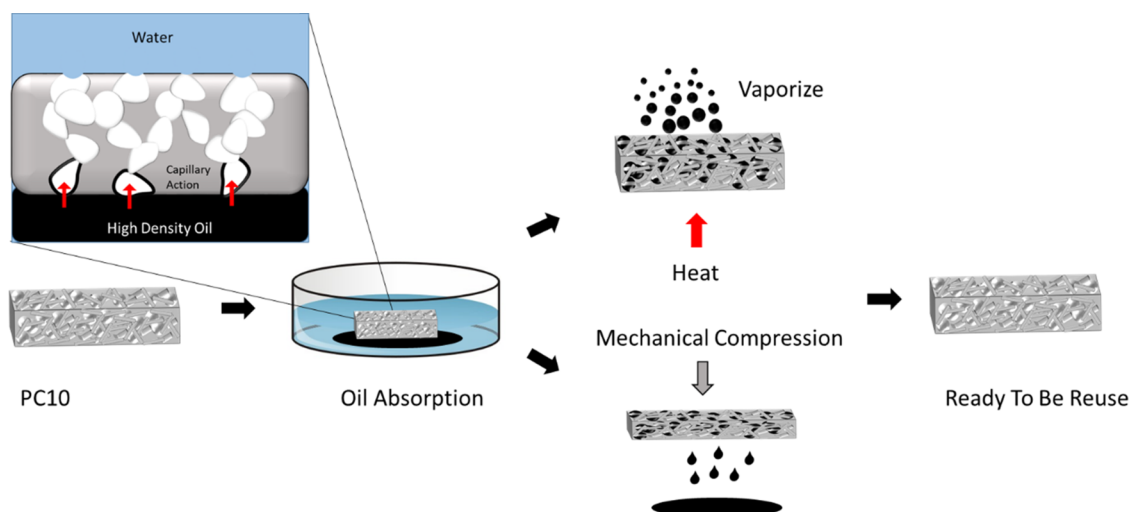
**Figure 9.** Schematic of recyclability of PDMS−CNT using heat and compression methods. Inset: Illustration oil uptake using PDMS−CNT.

static image of droplets of water on the surface. Contact angles on both sides were taken, and the average was calculated to determine the contact angle of the surface.

**Oil Absorption Test.** To determine the oil absorption capacity, initial mass, ($m_i$) of PDMS−CNT was obtained before being immersed in the oil or organic solvents (100 mL) until fully absorbed. After it was submerged, the surface residual liquid was drained before measuring the final mass, ($m_f$). Absorption capacity percentage was calculated using the following equation

$$q = \frac{m_f - m_i}{m_i} \times 100\% \tag{2}$$

Absorbates tested were petrol, diesel oil, engine oil, vegetable oil, toluene, cyclohexane, chlorobenzene, dichloromethane, and chloroform.

**Reproducibility, Recyclability, and Reusability Performance Test.** The absorbent was fabricated five more times to ensure reproducibility under similar condition and parameter. Reproducibility was verified with oil absorption test. Two methods of removing the absorbate were carried out: heat application and mechanical compression, as demonstrated in Figure 9. Heat application was performed using a hot plate to increase the temperature to the boiling point of the absorbate for removal through evaporation, whereas mechanical compression was performed by squeezing the PC10 to 10% of its original volume.

## ■ ASSOCIATED CONTENT

**ⓢ Supporting Information**

The Supporting Information is available free of charge on the ACS Publications website at DOI: 10.1021/acsome-ga.8b01566.

FESEM images of lower concentrations used in developing PDMS−CNT, surface wetting mechanism, detailed comparison of previous work (PDF), and short clip of selective absorption of chloroform dyed with Sudan III

(AVI)

## ■ AUTHOR INFORMATION

**Corresponding Author**

*E-mail: shuaib.saheed@utp.edu.my. Tel: +605-3687653.

**ORCID** ⓘ

Mohamed Shuaib Mohamed Saheed: 0000-0002-4620-889X

**Notes**

The authors declare no competing financial interest.

## ■ ACKNOWLEDGMENTS

## ■ REFERENCES

(1) Ingersoll, C.; Locke, R. M.; Reavis, C. BP and the Deepwater Horizon Disaster of 2010 *MIT Sloan Manage. Rev.* **2012**, *44*.

(2) Bovio, E.; Gnavi, G.; Prigione, V.; Spina, F.; Denaro, R.; Yakimov, M.; Calogero, R.; Crisafi, F.; Varese, G. C. The culturable mycobiota of a Mediterranean marine site after an oil spill: Isolation, identification and potential application in bioremediation. *Sci. Total Environ.* **2017**, *576*, 310−318.

(3) Tai, M. H.; Tan, B. Y. L.; Juay, J.; Sun, D. D.; Leckie, J. O. A self-assembled superhydrophobic electrospun carbon-silica nanofiber sponge for selective removal and recovery of oils and organic solvents. *Chem. - Eur. J.* **2015**, *21*, 5395−5402.

(4) Stolz, A.; Le Floch, S.; Reinert, L.; Ramos, S. M. M.; Tuaillon-Combes, J.; Soneda, Y.; Chaudet, P.; Baillis, D.; Blanchard, N.; Duclaux, L.; San-Miguel, A. Melamine-derived carbon sponges for oil-water separation. *Carbon* **2016**, *107*, 198−208.

(5) Cho, E. C.; Chang-Jian, C. W.; Hsiao, Y. S.; Lee, K. C.; Huang, J. H. Interfacial engineering of melamine sponges using hydrophobic TiO₂ nanoparticles for effective oil/water separation. *J. Taiwan Inst. Chem. Eng.* **2016**, *67*, 476−483.

(6) Zhang, W.; Lu, X.; Xin, Z.; Zhou, C. A self-cleaning polybenzoxazine/TiO₂ surface with superhydrophobicity and super-oleophilicity for oil/water separation. *Nanoscale* **2015**, *7*, 19476−19483.

(7) Mahadik, S. A.; Pedraza, F.; Parale, V. G.; Park, H. H. Organically modified silica aerogel with different functional silylating agents and effect on their physico-chemical properties. *J. Non-Cryst. Solids* **2016**, *453*, 164−171.

(8) Hu, H.; Zhao, Z.; Gogotsi, Y.; Qiu, J. Compressible Carbon Nanotube-Graphene Hybrid Aerogels with Superhydrophobicity and

Superoleophilicity for Oil Sorption. *Environ. Sci. Technol. Lett.* **2014**, *1*, 214−220.

(9) Li, Y.; Zhang, R.; Tian, X.; Yang, C.; Zhou, Z. Facile synthesis of $Fe_3O_4$ nanoparticles decorated on 3D graphene aerogels as broad-spectrum sorbents for water treatment. *Appl. Surf. Sci.* **2016**, *369*, 11−18.

(10) Hong, J. Y.; Sohn, E. H.; Park, S.; Park, H. S. Highly-efficient and recyclable oil absorbing performance of functionalized graphene aerogel. *Chem. Eng. J.* **2015**, *269*, 229−235.

(11) Yang, W.; Gao, H.; Zhao, Y.; Bi, K.; Li, X. Facile preparation of nitrogen-doped graphene sponge as a highly efficient oil absorption material. *Mater. Lett.* **2016**, *178*, 95−99.

(12) Ge, B.; Zhang, Z.; Zhu, X.; Men, X.; Zhou, X.; Xue, Q. A graphene coated cotton for oil/water separation. *Compos. Sci. Technol.* **2014**, *102*, 100−105.

(13) Fu, C.; Wang, Z.; Liu, J.; Jiang, H.; Li, G.; Zhi, C. Large scale fabrication of graphene for oil and organic solvent absorption. *Prog. Nat. Sci.: Mater. Int.* **2016**, *26*, 319−323.

(14) Niu, Z.; Chen, J.; Hng, H. H.; Ma, J.; Chen, X. A leavening strategy to prepare reduced graphene oxide foams. *Adv. Mater.* **2012**, *24*, 4144−4150.

(15) Gui, X.; Wei, J.; Wang, K.; Cao, A.; Zhu, H.; Jia, Y.; Shu, Q.; Wu, D. Carbon nanotube sponges. *Adv. Mater.* **2010**, *22*, 617−621.

(16) Gui, X.; Zeng, Z.; Lin, Z.; Gan, Q.; Xiang, R.; Zhu, Y.; Cao, A.; Tang, Z. Magnetic and highly recyclable macroporous carbon nanotubes for spilled oil sorption and separation. *ACS Appl. Mater. Interfaces* **2013**, *5*, 5845−5850.

(17) Tai, M. H.; Tan, B. Y. L.; Juay, J.; Sun, D. D.; Leckie, J. O. A self-assembled superhydrophobic electrospun carbon-silica nanofiber sponge for selective removal and recovery of oils and organic solvents. *Chem. - Eur. J.* **2015**, *21*, 5395−5402.

(18) Wu, L.; Li, L.; Li, B.; Zhang, J.; Wang, A. Magnetic, durable, and superhydrophobic polyurethane@$Fe_3O_4$@$SiO_2$@fluoropolymer sponges for selective oil absorption and oil/water separation. *ACS Appl. Mater. Interfaces* **2015**, *7*, 4936−4946.

(19) Choi, S.-J.; Kwon, T.-H.; Im, H.; Moon, D.-I.; Baek, D. J.; Seol, M.-L.; Duarte, J. P.; Choi, Y.-K. A Polydimethylsiloxane (PDMS) Sponge for the Selective Absorption of Oil from Water. *ACS Appl. Mater. Interfaces* **2011**, *3*, 4552−4556.

(20) Zhao, X.; Li, L.; Li, B.; Zhang, J.; Wang, A. Durable superhydrophobic/superoleophilic PDMS sponges and their applications in selective oil absorption and in plugging oil leakages. *J. Mater. Chem. A* **2014**, *2*, 18281−18287.

(21) Gui, X.; Li, H.; Wang, K.; Wei, J.; Jia, Y.; Li, Z.; Fan, L.; Cao, A.; Zhu, H.; Wu, D. Recyclable carbon nanotube sponges for oil absorption. *Acta Mater.* **2011**, *59*, 4798−4804.

(22) Hashim, D. P.; Narayanan, N. T.; Romo-Herrera, J. M.; Cullen, D. A.; Hahm, M. G.; Lezzi, P.; Suttle, J. R.; Kelkhoff, D.; Muñoz-Sandoval, E.; Ganguli, S.; Roy, A. K.; Smith, D. J.; Vajtai, R.; Sumpter, B. G.; Meunier, V.; Terrones, H.; Terrones, M.; Ajayan, P. M. Covalently bonded three-dimensional carbon nanotube solids via boron induced nanojunctions. *Sci. Rep.* **2012**, *2*, No. 363.

(23) Beshkar, F.; Khojasteh, H.; Salavati-niasari, M. Recyclable magnetic superhydrophobic straw soot sponge for highly efficient oil/water separation. *J. Colloid Interface Sci.* **2017**, *497*, 57−65.

(24) Gupta, S.; Tai, N.-H. Carbon materials as oil sorbents: a review on the synthesis and performance. *J. Mater. Chem. A* **2016**, *4*, 1550−1565.

(25) Nour, M.; et al. CNT / PDMS composite membranes for $H_2$ and $CH_4$ gas separation. *Int. J. Hydrogen Energy* **2013**, *38*, 10494−10501.

(26) Maji, D.; Lahiri, S. K.; Das, S. Study of hydrophilicity and stability of chemically modified PDMS surface using piranha and KOH solution. *Surf. Interface Anal.* **2012**, *44*, 62−69.

(27) Agarwal, R.; Tandon, P.; Gupta, V. D. Phonon dispersion in poly(dimethylsilane). *J. Organomet. Chem.* **2006**, *691*, 2902−2908.

(28) Bodas, D.; Khan-Malek, C. Formation of more stable hydrophilic surfaces of PDMS by plasma and chemical treatments. *Microelectron. Eng.* **2006**, *83*, 1277−1279.

(29) Jamal, G. R. A.; Mominuzzaman, S. M. Different Techniques for Chirality Assignment of Single Wall Carbon Nanotubes. *J. Nanosci. Nanoeng.* **2015**, *1*, 74−83.

(30) Bertoncini, M.; Coelho, L. A. F.; Maciel, I. O.; Pezzin, S. H. Purification of Single-Wall carbon nanotubes by heat treatment and supercritical extraction. *Mater. Res.* **2011**, *14*, 380−383.

(31) Atieh, M. A.; Bakather, O. Y.; Al-Tawbini, B.; Bukhari, A. A.; Abuilaiwi, F. A.; Fettouhi, M. B. Characterization of carbon nanotubes by Raman spectroscopy. *Bioinorg. Chem. Appl.* **2010**, *2010*, 1−9.

(32) Al-zubaidi, A.; Ishii, Y.; Yamada, S.; Matsushita, T.; Kawasaki, S. Spectroscopic evidence for the origin of the dumbbell cyclic voltammogram of single-walled carbon nanotubes. *Phys. Chem. Chem. Phys.* **2013**, *15*, 20672−20678.

(33) Zisman, W. A. Contact Angle, Wettability, and Adhesion; Advances in Chemistry. In *Relation of the Equilibrium Contact Angle to Liquid and Solid Constitution*; American Chemical Society, 1964; Vol. *43*, pp 1−51.

(34) Bracco, G.; Holst, B. Contact Angle and Wetting Properties. In *Surface Science Techniques*; Springer: New York, 2013; Vol. *51*, pp 1−34.

(35) Kubiak, K. J.; Wilson, M. C. T.; Mathia, T. G.; Carval, P. Wettability versus roughness of engineering surfaces. *Wear* **2011**, *271*, 523−528.